

# Knockdown of end-binding protein 1 induces apoptosis in radioresistant A549 lung cancer cells via p38 kinase-dependent COX-2 upregulation

JEONG-HWA BAEK<sup>1,2\*</sup>, JI-HYE YIM<sup>1\*</sup>, JIE-YOUNG SONG<sup>1</sup>, HONG-DUCK UM<sup>1</sup>, JONG KUK PARK<sup>1</sup>, IN-CHUL PARK<sup>1</sup>, JAE-SUNG KIM<sup>1</sup>, CHANG-WOO LEE<sup>2</sup>, EUN-HEE HONG<sup>3</sup>, EUN HO KIM<sup>1\*\*</sup> And SANG-GU HWANG<sup>1\*\*</sup>

<sup>1</sup>Division of Applied Radiation Bioscience, Korea Institute of Radiological and Medical Sciences, Seoul 01812;

<sup>2</sup>Department of Molecular Cell Biology, Sungkyunkwan University School of Medicine, Suwon 440-746;

<sup>3</sup>Low-dose Radiation Research Team, Korea Hydro and Nuclear Power, Seoul 01450, Republic of Korea

Received October 7, 2017; Accepted February 12, 2018

DOI: 10.3892/or.2018.6278

**Abstract.** The role of end-binding protein 1 (EB1) in lung cancer tumorigenesis and radiotherapy remains poorly understood. In the present study, we observed that EB1 was highly expressed in lung tumor tissues compared with normal non-tumor tissues based on immunohistochemical analysis of lung cancer tissue samples obtained from human tissue microarrays. EB1 was also highly overexpressed in radioresistant lung and cervical cancer cells, which exhibited increased cell death after EB1 silencing. The cytotoxicity induced by EB1 gene knockdown was due to the activation and generation of reactive oxygen species by p38 mitogen-activated protein kinase. Notably, this signaling cascade, however not nuclear factor- $\kappa$ B-mediated signaling, induced the expression of cyclooxygenase-2, a key effector of apoptotic death. Our results provided new molecular evidence supporting the use of EB1 as a novel target in lung cancer therapy, especially in the case of radioresistance.

## Introduction

Human end-binding protein 1 (EB1), a member of the plus-end-tracking protein family that was originally reported in colorectal cancer (1), regulates microtubule dynamics

by promoting microtubule growth and suppressing catastrophes (2). Subsequently, EB1 overexpression has been reported in gastric and hepatic cancers according to proteomic analysis (3,4) and in oral cancer based on liquid chromatography-mass spectrometry (5). These observations indicated that EB1 can serve as a biomarker for tumor progression. The oncogenic function of EB1 has been experimentally observed in esophageal, breast and glioblastoma cancer cells. EB1 promotes tumor cell proliferation by activating Wnt signaling (6), which indicates that it is a marker of poor prognosis. In addition, EB1 regulates the migration of B16F1 melanoma cells by modulating the balance between lamellipodia and filopodia protrusions (7). Previously, we reported that EB1 was a biomarker of radioresistance in non-small cell lung carcinoma (NSCLC) (8). Although several studies elucidating EB1 function have been performed using different human tumor tissues, the precise role of EB1 and its molecular mechanism of action related to cytotoxicity in cancer remains to be elucidated.

Cyclooxygenase-2 (COX-2) is a rate-limiting enzyme in arachidonic acid metabolism and is responsible for regulating inflammation, pain and angiogenesis (9). The first genetic evidence for the association between COX-2 and carcinogenesis was obtained for colorectal cancer and the potential chemotherapeutic role of COX-2 inhibitors has been demonstrated in numerous types of cancer (10,11). Conversely, COX-2 overexpression inhibited the cell cycle and tumor progression in osteosarcoma cells (12). Although our previous study revealed that EB1 knockdown promoted reactive oxygen species (ROS)-induced apoptosis in NSCLC cells via nuclear factor- $\kappa$ B (NF- $\kappa$ B) activation (8), the correlation between COX-2 and NSCLC cell death and the association between COX-2 regulation and EB1 remain unclear.

Therefore, in the present study, we aimed to elucidate the mechanisms regulating ROS production and COX-2 expression in EB1-knockdown lung cancer cells. In the present study we provided further molecular evidence supporting the potential application of EB1 as a novel target related to radioresistance in lung cancer gene therapy.

---

*Correspondence to:* Dr Sang-Gu Hwang or Dr Eun Ho Kim, Division of Applied Radiation Bioscience, Korea Institute of Radiological and Medical Sciences, 75 Nowon-ro, Nowon-gu, Seoul 01812, Republic of Korea  
E-mail: sgh63@kccch.re.kr  
E-mail: eh140149@kirams.re.kr

\*\*Contributed equally

**Key words:** A549 lung cancer cells, COX-2, EB1, MAPKs, radioresistance, ROS

## Materials and methods

**Cell culture and treatment.** Human A549 lung cancer and SiHa and HeLa cervical cancer cell lines were purchased from the American Type Culture Collection (ATCC; Manassas, VA, USA). A549 cells were cultured in RPMI-1640 medium and SiHa and HeLa cells were cultured in Dulbecco's modified Eagle's medium (DMEM; Gibco® Life Technologies, Carlsbad, CA, USA) supplemented with 10% fetal bovine serum (FBS; Gibco®, Life Technologies). The cells were irradiated using a <sup>137</sup>Cs source (Atomic Energy of Canada, Ltd., Mississauga, ON, Canada) at a dose rate 3.81 Gy/min and treated with 10 mM N-acetyl cysteine (NAC; Sigma-Aldrich; Merck KGaA, Darmstadt, Germany) to scavenge ROS, 1 μM BAY 11-7082 (BAY) to inhibit NF-κB activity and 20 μM SB203580 (SB) (both from Calbiochem; Merck KGaA), to inhibit p38 kinase, or 10 μM cycloheximide (CHX; Sigma-Aldrich; Merck KGaA) to block *de novo* protein synthesis.

**Cell death assay.** Cell death was assessed as previously described (8). Apoptotic death was also determined by alterations in cellular morphology.

**Quantitative reverse transcription-polymerase chain reaction (qRT-PCR).** Transcripts were quantified by qRT-PCR as previously described (13) using the following primer pairs: EB1 (333-bp product) 5'-CTGCGTATTGTCAGTTTATG-3' (sense) and 5'-GAGGTTTCTTCGGTTTATTC-3' (antisense); COX-2 (580-bp product), 5'-CTGGCGCTCAGCCATACAGC-3' (sense) and 5'-GGCCCTCGCTTATGATCTGTC-3' (antisense); and glyceraldehyde-3-phosphate dehydrogenase (GAPDH; 305-bp product), 5'-CATCTCTGCCCCCTCTGCTGA-3' (sense) and 5'-GGATGACCTTGCCACAGCCT-3' (antisense).

**Oncomine data mining.** Oncomine (Life Technologies; Thermo Fisher Scientific, Inc., Waltham, MA, USA) was used for data analysis and visualization as previously described (14). The expression of EB1 was compared between lung cancer and normal lung tissue extracts.

**Immunohistochemistry.** Human tissue microarrays were purchased from SuperBioChips (cat. no. CC5; Seoul, Korea) and immunohistochemistry was performed using an anti-EB1 mouse monoclonal antibody (dilution, 1:250; cat. no. sc-47704; Santa Cruz Biotechnology, Inc., Santa Cruz, CA, USA) as previously described (15). Immunostaining was performed using the avidin-biotin-peroxidase method according to the manufacturer's instructions (Vector Laboratories, Burlingame, CA, USA). Staining intensity was scored as follows: 0, no visible staining; 1+, weak staining; 2+, moderate staining; 3+, strong staining; and 4+, very strong staining.

**Knockdown of proteins by small interference RNA (siRNA).** The following human-specific siRNAs synthesized following the manufacturer's instructions (Genolution, Inc., Seoul, Korea) were used: siEB1, 5'-UUGCCUUGAAGAAAGUGA AUU-3' (sense) and 5'-UUCACUUUCUUAAGGCAAUU-3' (antisense); sip38, 5'-GAAGCUCUCCAGACCAUUUUU-3' (sense) and 5'-AAAUGGUCUGGAGAGCUUCU-3' (antisense); and siCOX-2, 5'-AACUGCUCACACCGGAAUUU

UUUU-3' (sense) and 5'-AAAAAUCCGGUGUUGAGCAG UUUU-3' (antisense). A scrambled siRNA that exhibited no significant homology to known gene sequences was used as a negative control. The cells were transfected with 30 nM siRNA in medium, as previously described (13).

**ROS assay.** The cells were incubated with 10 nM 2',7'-dichlorofluorescein diacetate; Molecular Probes, Inc., Eugene, OR, USA) for 20 min to detect ROS, as previously described (8).

**Immunofluorescence confocal microscopy.** Immunofluorescence staining for EB1 (Santa Cruz Biotechnology, Inc.) and COX-2 (Cayman Chemical, Ann Arbor, MI, USA) was performed as previously described (8). Cell nuclei were identified by staining with 4,6-diamidino-2-phenylindole (DAPI).

**Western blot analysis.** Western blot analysis were performed as previously described (13) using primary antibodies against the following: EB1 (cat. no. sc-47704), p53 (cat. no. sc-126), IκB (cat. no. sc-371), phospho-ERK (cat. no. sc-7383) and p38 (cat. no. sc-535) (all from Santa Cruz Biotechnology, Inc.); cleaved PARP (Asp214, cat. no. 9541), phospho-p53 (Ser15, cat. no. 9284), phospho-JNK (cat. no. 9251), JNK (cat. no. 9252), phospho-p38 (cat. no. 9211) and ERK (cat. no. 9102) were obtained from Cell Signaling Technology Inc. (Beverly, MA, USA) and COX-2 (cat. no. 160106) from Cayman Chemical. β-actin (A1978; Sigma-Aldrich; Merck KGaA) was used as a loading control. Blots were reacted with primary antibodies at dilution, 1:1,000 and secondary antibodies at dilution, 1:5,000.

**Statistical analysis.** Cell culture experiments were repeated at least three times. All data are expressed as the mean ± standard deviation (SD). Statistical differences between groups were assessed by the Student's t-test and Bonferroni's multiple comparison test. P<0.05 was considered to indicate a statistically significant difference.

## Results

**EB1 protein as a radioresistance and tumorigenesis biomarker in NSCLC.** As displayed in Fig. 1A, treatment with 10 Gy radiation induced cell death in ~63% H460 vs. 26% A549 lung cancer cells, 65% parental H460 vs. 33% artificially established R-H460 cells and 66% HeLa vs. 30% SiHa cervical cancer cells at 72 h post-stimulation. Although the mRNA level remained unchanged between the parental H460 and R-H460 cells, both EB1 protein and mRNA were highly overexpressed in the radioresistant A549, R-H460 and SiHa cell lines compared with the radiosensitive H460 and HeLa cancer cells (Fig. 1B). This observation indicated that EB1 could serve as a biomarker for radioresistance. qRT-PCR data revealed that EB1 mRNA levels in A549 and SiHa cells increased by ~2.9- and 2.2-fold compared with that in H460 and HeLa cells, respectively (Fig. 1C). Subsequently, the correlation between EB1 expression and lung cancer severity was examined using the human genetic dataset analysis tool Oncomine. EB1 mRNA levels were markedly increased in lung adenocarcinoma tumors (Fig. 1D) compared with normal lung tissues, indicating that EB1 is also a tumorigenesis factor.

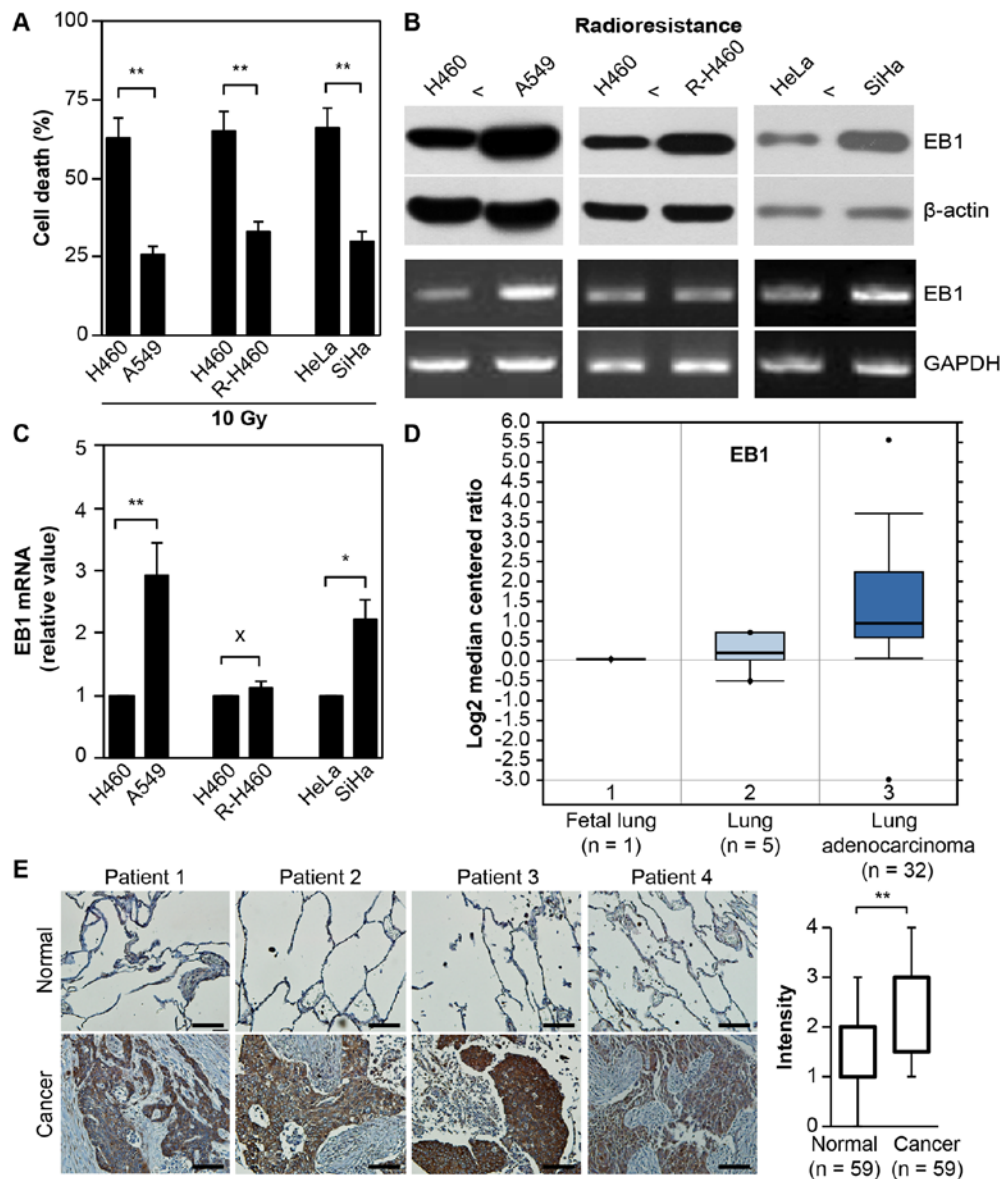


Figure 1. EB1 protein as a radioresistance and tumorigenesis biomarker. (A) Lung and cervical cancer cell lines were treated with 10 Gy radiation for 48 h. Cell death was determined by FACS analysis and the data are expressed as the mean  $\pm$  SD (\*\* $P < 0.005$  compared with radiosensitive control cells). (B and C) Each cell line was cultured for 36 h without any stimulation. Protein and transcription levels of EB1 were determined by western blot analysis (B, top panel) and conventional PCR (B, bottom panel; loading control, GAPDH), respectively. (C) The qRT-PCR data are expressed as the mean  $\pm$  SD (\*\* $P < 0.05$  and \*\*\* $P < 0.005$  compared with radiosensitive control cells; X denotes no significance compared with control cells). (D) Available datasets in the Oncomine database were queried for EB1 expression with respect to cancer vs. normal tissue (threshold  $P$ -value =  $3.87 \times 10^{-4}$ ; fold-change  $\geq 2$ ). (E) Representative microscopic images of lung cancer tissues and their normal tissue counterparts stained with an anti-EB1 antibody (left panel, scale bar, 50  $\mu$ m). Staining intensity scored as follows in all tissue samples (n=59): 0, no staining; +1, weak; +2, moderate; +3, strong; and +4, very strong. The data are presented as box and whisker plots. \*\* $P < 0.005$  compared with the staining intensity of normal tissues. EB1, end-binding protein 1; FACS, fluorescence-activated cell sorting; SD, standard deviation; qPCR, quantitative polymerase chain reaction; GAPDH, glyceraldehyde-3-phosphate dehydrogenase.

Consistent with the Oncomine data, *in vivo* evidence based on tissue microarrays for lung cancer and normal tissues revealed considerably upregulated EB1 expression in lung cancer tissues compared with normal tissues. Representative images of lung cancer and normal tissues are shown in Fig. 1E; for the intensity calculation, all tissue data were analyzed. These results indicated that EB1 induction may play an important role in the acquisition of the radioresistant phenotype and tumorigenesis in H460 cells.

*EB1 depletion promotes p38 kinase-dependent ROS-mediated apoptosis in A549 NSCLC cells.* We have previously reported

EB1 depletion-mediated accumulation of ROS in A549 cells, although the upstream activator of ROS production could not be determined (8). In the present study, we observed that EB1 depletion in A549 cells markedly induced p38 kinase activity, but not that of ERK or JNK, without inducing any change in basal protein levels (Fig. 2A). Furthermore, as determined by cell staining (Fig. 2B and C, top panel), inhibition of p38 kinase using a p38-specific siRNA (Fig. 2B) or the chemical inhibitor SB203580 (Fig. 2C) almost completely reduced ROS levels, which accumulated due to EB1 depletion. In addition, fluorescence-activated cell sorting (FACS) analysis revealed that ROS levels were increased by  $\sim 1.98$ -fold in EB1-depleted

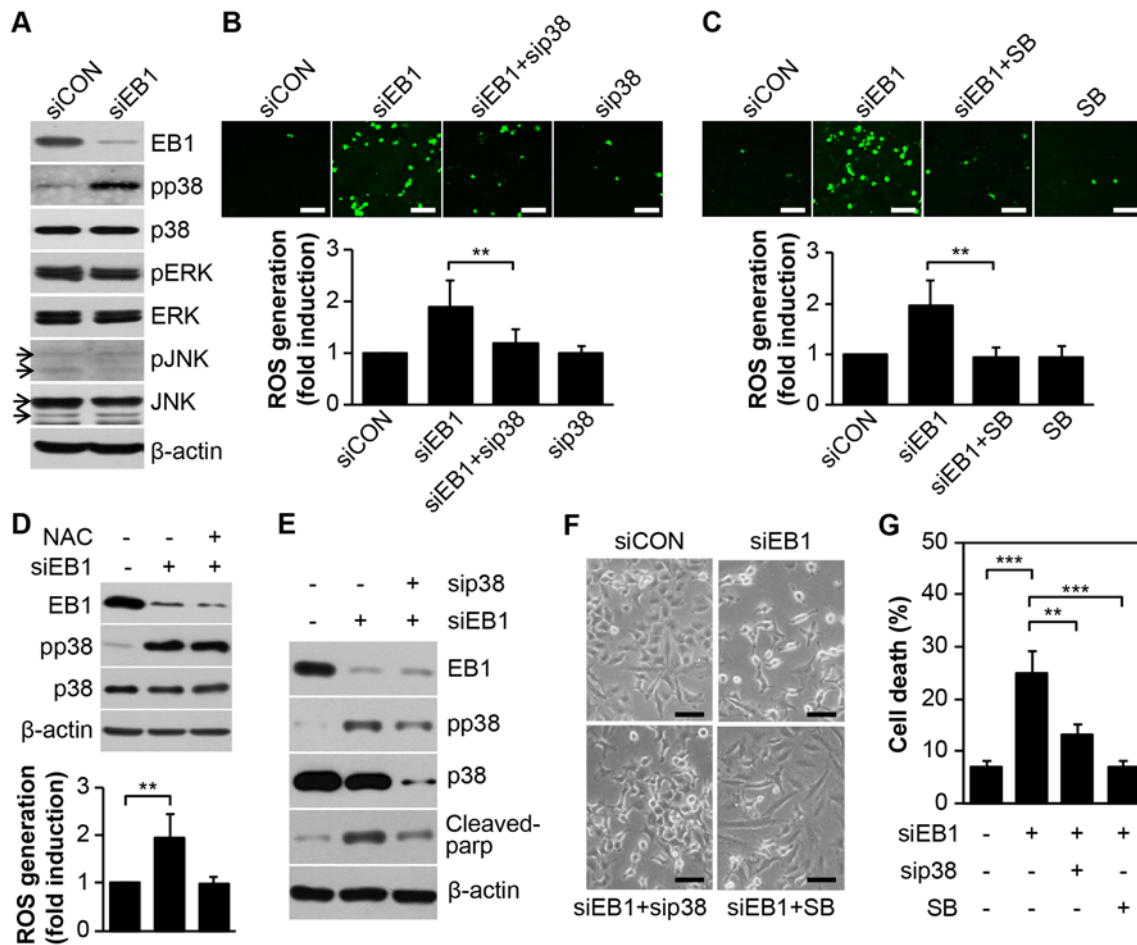


Figure 2. EB1 depletion promotes p38 kinase activation-dependent ROS generation to induce A549 cancer cell death. (A) A549 cells were transfected with 30 nM control siRNA (siCON) or EB1 siRNA (siEB1) for 36 h. Protein and phosphorylation levels of EB1 and MAPKs were determined by western blot analysis. (B) A549 cells were transfected with 30 nM siCON, EB1 siRNA and/or p38 siRNA (sip38) for 36 h. Intracellular ROS levels were assessed by confocal microscopy (top panel, scale bar, 0.1 mm) and determined by FACS analysis. The data are expressed as the mean  $\pm$  SD (\*\* $P$ <0.005 compared with siEB1-transfected cells, bottom graph). (C) A549 cells were transfected with 30 nM siCON or EB1 siRNA for 36 h in the absence or presence of 20  $\mu$ M SB203580 (SB). Intracellular ROS levels were determined as noted in B. (D) A549 cells were transfected as described in A in the absence or presence of 10 mM NAC. Protein and phosphorylation levels of EB1 and p38 kinase were determined by western blot analysis (top panel). ROS production was assessed by FACS analysis. The data are expressed as the mean  $\pm$  SD (\*\* $P$ <0.005 compared with siEB1 alone-transfected cells, bottom graph). (E-G) A549 cells were transfected as mentioned in B and C. Protein levels of EB1, p38 and cleaved PARP and phosphorylation level of p38 were determined by (E) western blot analysis. Morphological changes were observed by (F) light microscopy (scale bar, 0.1 mm) and cell death was determined by (G) FACS analysis. The data are expressed as the mean  $\pm$  SD (\*\* $P$ <0.005 compared with siEB1-transfected cells) (G). EB1, end-binding protein 1; MAPK, mitogen-activated protein kinase; ROS, reactive oxygen species; FACS, fluorescence-activated cell sorting; SD, standard deviation; PARP, poly(ADP-ribose) polymerase.

A549 cells and  $\sim$ 1.21- and 1.01-fold in p38 siRNA- and SB203580-stimulated A549 cells, respectively, compared with the levels in control cells (Fig 2B and C, bottom panel). However, inhibition of ROS generation using a ROS scavenger (NAC) did not alter p38 kinase activity in EB1-depleted A549 cells (Fig. 2D), indicating that p38 kinase is involved in ROS production due to siEB1. Subsequently, we used a p38 loss-of-function approach to examine whether the p38 kinase-induced ROS cascade is critical for siEB1-mediated A549 cell death. Notably, the reduction in p38 kinase protein due to a p38-specific siRNA markedly suppressed cleaved PARP levels, which was significantly induced by an increase in p38 phosphorylation in EB1-knockdown A549 cells (Fig. 2E). Consistent with the biochemical results, cell morphology analysis also revealed a marked restoration of survival in EB1-depleted A549 cells after treatment with both p38 siRNA and SB203580 (Fig. 2F). FACS analysis revealed that cell death increased by  $\sim$ 3.6-fold in siEB1-treated A549 cells and  $\sim$ 1.9- and 1.1-fold in p38

siRNA- and SB203580-stimulated A549 cells, respectively, compared with that in control cells (Fig. 2G). Collectively, our data indicated that EB1-depleted A549 cell cytotoxicity was attributable to ROS generation through p38 kinase activation.

#### *Regulation of COX-2 expression is p38 kinase dependent but not NF- $\kappa$ B dependent in EB1-depleted A549 NSCLC cells.*

Given that the COX-2 enzyme plays critical roles in numerous biological processes, including inflammation, cancer cell death and development (16,17), we examined the correlation between COX-2 and EB1 knockdown-induced cytotoxicity in A549 cells. As displayed in Fig. 3A, silencing of EB1 in A549 cells markedly induced the expression of COX-2 protein (top panel) and transcript (middle panel), as determined by western blot analysis and conventional PCR analyses, respectively. qRT-PCR revealed that EB1 and COX-2 mRNA levels were reduced by  $\sim$ 80% and increased by  $\sim$ 2.21-fold, respectively, in EB1-depleted A549 cells compared with control cells

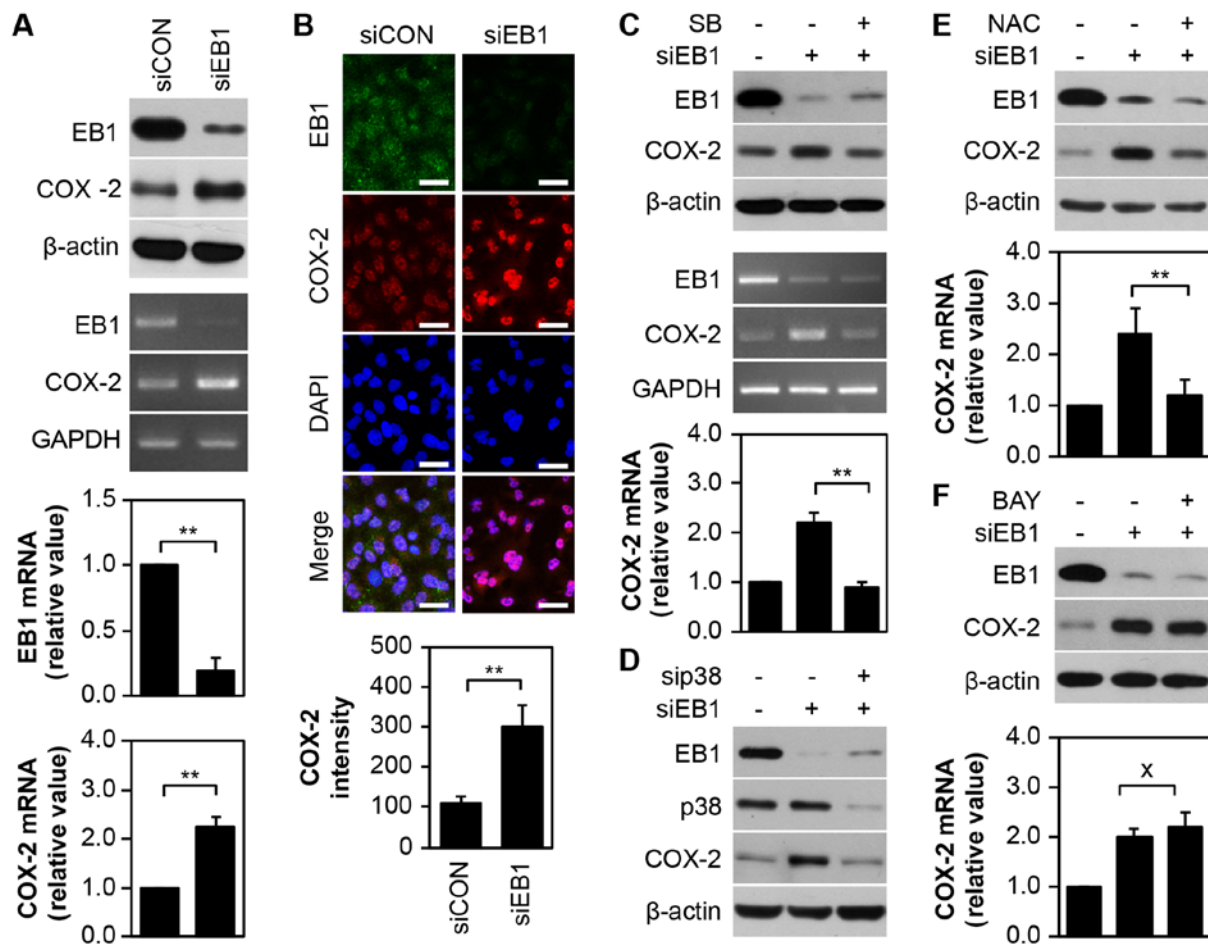


Figure 3. EB1 depletion upregulates the expression of COX-2 via p38-ROS signaling activation, but not the NF- $\kappa$ B pathway in A549 cancer cells. (A and B) A549 cells were transfected with 30 nM siCON or siEB1 for 36 h. Protein and transcription levels of EB1 and COX-2 were determined by western blot analysis (A, top panel) and conventional PCR (A, middle panel; loading control: GAPDH), respectively. The qRT-PCR (A, bottom panel) data are expressed as the mean  $\pm$  SD (\*\* $P$ <0.005 compared with control cells). (B, top panel) EB1 and COX-2 localization was visualized by confocal microscopy and representative images are shown (scale bar, 0.1 mm). (B, bottom panel). Quantification of the fluorescent area of the cells is expressed as the mean  $\pm$  SD (\*\* $P$ <0.005 compared with control cells). (C) A549 cells were transfected with 30 nM siCON or siEB1 for 36 h in the absence or presence of 20  $\mu$ M SB203580. Protein and transcription levels of EB1 and COX-2 were determined by western blot analysis (top panel) and conventional PCR (middle panel, loading control: GAPDH), respectively. The qRT-PCR data (bottom panel) are expressed as the mean  $\pm$  SD (\*\* $P$ <0.005 compared with siEB1 alone-transfected cells). (D) A549 cells were transfected with 30 nM siCON, siEB1 and/or sip38 for 36 h. EB1, p38 and COX-2 protein levels were determined by western blot analysis. (E and F) A549 cells were transfected with 30 nM siCON or siEB1 for 36 h in the absence or presence of 10 mM NAC (E) or 2  $\mu$ M Bay (F). EB1 and COX-2 protein levels were determined by western blot analysis (top panel) and COX-2 transcription levels were determined by qRT-PCR (bottom panel). The data are expressed as the mean  $\pm$  SD (\* $P$ <0.05 compared with siEB1 alone-transfected cells; x denotes no significance compared with siEB1-transfected cells). EB1, end-binding protein 1; COX-2, cyclooxygenase-2; ROS, reactive oxygen species; NF- $\kappa$ B nuclear factor- $\kappa$ B; GAPDH, glyceraldehyde-3-phosphate dehydrogenase; GAPDH, glyceraldehyde-3-phosphate dehydrogenase; qPCR, quantitative polymerase chain reaction; siCON, control siRNA; siEB1, EB1 siRNA.

(Fig. 2A, bottom panel). Although no significant alteration in nuclear COX-2 distribution dynamics was observed in A549 cells following EB1 knockdown (Fig. 3B, top panel), COX-2 expression surprisingly increased by ~3.02-fold compared with control cells. This result was consistent with the results of immunofluorescence confocal microscopy (Fig. 3B, bottom panel). However, in A549 cells, selective inhibition of p38 kinase with SB203580 decreased COX-2 protein (Fig. 3C, top panel) and transcription levels mediated by EB1 depletion (Fig. 3C, middle panel). qRT-PCR results also demonstrated similar levels of COX-2 mRNA in EB1-depleted SB203580-treated A549 cells and in unstimulated control cells (Fig. 3C, bottom panel). Additionally, inhibition of p38 kinase protein expression using a p38-specific siRNA considerably suppressed EB1 depletion-induced COX-2 expression in A549 cells (Fig. 3D), indicating that p38 kinase is an upstream

regulator of the expression of COX-2. The suppression of ROS in EB1-depleted A549 cells using NAC resulted in COX-2 expression patterns that were similar to those observed after p38 kinase inhibition (Fig. 3E), indicating that the p38-ROS signaling axis is a key player in COX-2 regulation. Although the COX-2 gene is a target of the transcription factor NF- $\kappa$ B, we observed that NF- $\kappa$ B inhibition using BAY 11-7082 (BAY) in EB1-knockdown A549 cells did not alter the high levels of COX-2 expression (Fig. 3F). This finding indicated that p38 kinase-dependent and NF- $\kappa$ B-independent COX-2 regulation is associated with EB1-mediated signaling.

*COX-2 plays a critical role in EB1 knockdown-mediated A549 NSCLC cell death.* Consistent with the results demonstrating overexpression of the COX-2 protein during EB1 depletion-induced A549 cell death (Fig. 4A, left panel), other

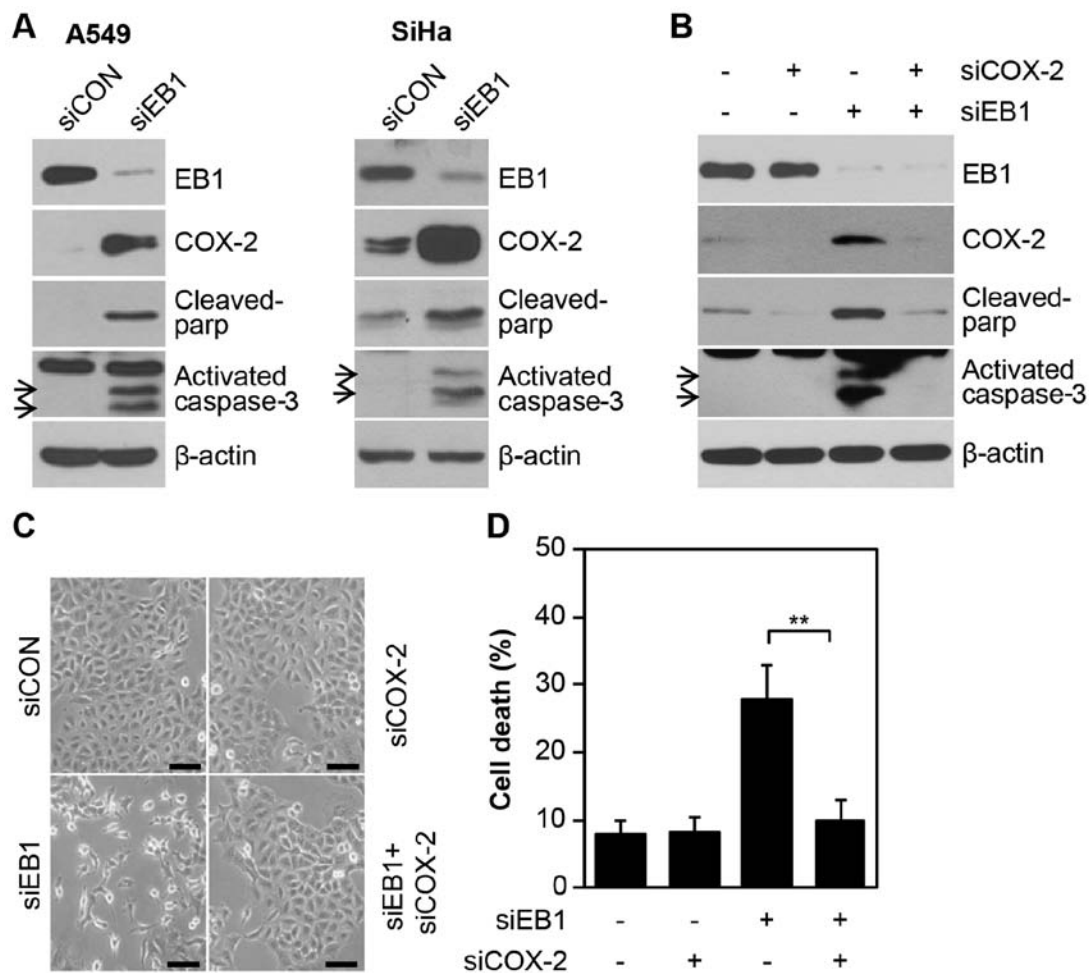


Figure 4. COX-2 induced by EB1 knockdown plays a critical role in A549 cancer cell death. (A) A549 (left panel) and SiHa (right panel) cells were transfected with 30 nM siCON or siEB1 for 36 h. EB1, COX-2, cleaved PAR and activated caspase-3 protein levels were determined by western blot analysis. (B-D) A549 cells were transfected with 30 nM siCON or siEB1 and/or COX-2 siRNA (siCOX-2) for 48 h. EB1, COX-2, cleaved PARP and activated caspase-3 protein levels were determined by western blot analysis. (B) Morphological changes were observed by (C) light microscopy (scale bar, 0.1 mm) and cell death was determined by (D) FACS analysis. The data are expressed as the mean  $\pm$  SD (\*\* $P$ <0.005 compared with siEB1-transfected cells). EB1, end-binding protein 1; COX-2, cyclooxygenase-2; siCON, control siRNA; siEB1, EB1 siRNA; PARP, poly(ADP-ribose) polymerase.

radioresistant cell lines, such as SiHa cervical cancer cells, also exhibited induction of COX-2 protein expression under the same conditions. In addition, two important apoptotic markers, cleaved PARP and activated caspase-3, were also increased (Fig. 4A) in EB1 depleted A549 and SiHa cell lines. This finding indicated the potential association between the overexpression of COX-2 and EB1 knockdown-mediated cell death. Furthermore, COX-2 levels could not be detected in control cells and were significantly stable (half-life, >9 h) in EB1-knockdown A549 cells treated with the translation inhibitor CHX, demonstrating that EB1 was involved in regulating COX-2 protein stability (data not shown). Finally, to establish the primary role of COX-2 in EB1 knockdown-mediated cell death, A549 cells were transfected with a COX-2-specific siRNA alone or in combination with EB1-specific siRNA. Notably, EB1 knockdown-induced A549 cell death was markedly reduced by direct inhibition of COX-2 expression, as determined by western blot analysis for two apoptotic markers (Fig. 4B). Data on changes in cell morphology also corroborated the above mentioned biochemical results (Fig. 4C). FACS analysis also demonstrated that cell death was increased to ~28.6% in siEB1-treated A549 cells and reduced to ~9.2% in

cells also transfected with COX-2 siRNA compared with ~8% in control cells (Fig. 4D). Collectively, our results indicated that COX-2 is essential for EB1-mediated regulation of the cell fate in different cell lines, including radioresistant A549 NSCLC cells. However, this observation may not be limited to lung cancer cells.

## Discussion

In the present study, we aimed to identify novel strategies for improving the response ratio of radiotherapy and to determine radioresistance factors in lung cancer cells. We have previously reported (8) that EB1 was involved in regulating tumor cell death leading to radioresistance and that EB1 knockdown promoted apoptosis in lung cancer cells by increasing expression of the pro-apoptotic protein Bax via ROS-dependent NF- $\kappa$ B activation (8). However, the molecular mechanisms and detailed pathways underlying radiation-induced resistance in lung cancer cells has remained a topic of further investigation. We performed the present study to explore the molecular mechanisms underlying EB1-mediated inhibition of tumor cell cytotoxicity following exposure to radiation. We observed that

the mechanisms underlying this effect involved EB1 depletion, which promoted p38 kinase-dependent ROS-mediated apoptosis in A549 cells. This p38-dependent apoptosis was critical for upregulating COX-2.

Given that MAPKs are central mediators of cell death and survival pathways and are implicated in the response of tumor cells to diverse antitumor signals, including radiation, we first investigated the MAPK signaling pathway (18). EB1 silencing in A549 cells significantly induced p38 phosphorylation. However, ERK and JNK were not activated. Previously, our group demonstrated that downregulation of EB1 is related to NF- $\kappa$ B-dependent signaling cascades. In the present study, NF- $\kappa$ B, another known transcriptional regulator of COX-2, was not found to be involved in the increase of COX-2 via the EB1-p38-COX-2 signaling axis. Several studies have suggested the involvement of COX-2 in tumor progression and carcinogenesis and different protein kinase-mediated pathways regulate COX-2 expression in response to different cellular stress signals (16). Although COX-2 modulates cell proliferation or apoptosis in several solid tumors, its functions appear to be controversial (17). Thus, COX-2 modulation is a promising field investigated by numerous research groups. Our results indicated that COX-2 is essential for EB1 knockdown-mediated A549 cell death. We demonstrated that the upregulation of COX-2 in EB1-depleted cells required the activation of the p38 MAPK pathway and led to apoptosis.

In conclusion, we revealed in the present study that EB1 knockdown in radioresistant lung cancer cells (A549) relied on the signaling pathway leading to p38-dependent COX-2 upregulation, which ultimately induced ROS-mediated apoptosis. Our results also indicated that knockdown of EB1 may effectively improve the therapeutic effects of RT in patients with radioresistant lung cancer. Therefore, a better understanding of the potential molecular mechanisms underlying the radioresistance effect of EB1 is of immense importance in lung cancer research and radiation therapy. Collectively, our results indicated that EB1 could be used as a biomarker for RT.

#### Acknowledgments

Not applicable.

#### Funding

The present study was supported by a grant from the Korea Institute of Radiological and Medical Sciences (KIRAMS) funded by the Ministry of Science and ICT (MSIT), Republic of Korea (50531-2018).

#### Availability of data and materials

The datasets used during the present study are available from the corresponding author upon reasonable request.

#### Authors' contributions

SGH, EHK conceived the idea, designed the experiment setup and wrote the manuscript. JHB, JHY and EHH performed the experiments. SGH, EHK analysed the data. JYS, HDU, JKP, ICP, JSK and CWL discussed the data. All authors read and

approved the manuscript and agree to be accountable for all aspects of the research in ensuring that the accuracy or integrity of any part of the work are appropriately investigated and resolved.

#### Ethics approval and consent to participate

Not applicable.

#### Consent for publication

Not applicable.

#### Competing interests

The authors declare that they have no competing interests.

#### References

- Orimo T, Ojima H, Hiraoka N, Saito S, Kosuge T, Kakisaka T, Yokoo H, Nakanishi K, Kamiyama T, Todo S, *et al*: Proteomic profiling reveals the prognostic value of adenomatous polyposis coli-end-binding protein 1 in hepatocellular carcinoma. *Hepatology* 48: 1851-1863, 2008.
- Kumar M, Mehra S, Thakar A, Shukla NK, Roychoudhary A, Sharma MC, Ralhan R and Chauhan SS: End Binding 1 (EB1) overexpression in oral lesions and cancer: A biomarker of tumor progression and poor prognosis. *Clin Chim Acta* 459: 45-52, 2016.
- Wang Y, Zhou X, Zhu H, Liu S, Zhou C, Zhang G, Xue L, Lu N, Quan L, Bai J, *et al*: Overexpression of EB1 in human esophageal squamous cell carcinoma (ESCC) may promote cellular growth by activating beta-catenin/TCF pathway. *Oncogene* 24: 6637-6645, 2005.
- Dong X, Liu F, Sun L, Liu M, Li D, Su D, Zhu Z, Dong JT, Fu L and Zhou J: Oncogenic function of microtubule end-binding protein 1 in breast cancer. *J Pathol* 220: 361-369, 2010.
- Berges R, Baeza-Kallegre N, Tabouret E, Chinot O, Petit M, Kruczynski A, Figarella-Branger D, Honore S and Braguer D: End-binding 1 protein overexpression correlates with glioblastoma progression and sensitizes to Vinca-alkaloids in vitro and in vivo. *Oncotarget* 5: 12769-12787, 2014.
- Nishigaki R, Osaki M, Hiratsuka M, Toda T, Murakami K, Jeang KT, Ito H, Inoue T and Oshimura M: Proteomic identification of differentially-expressed genes in human gastric carcinomas. *Proteomics* 5: 3205-3213, 2005.
- Schober JM, Cain JM, Komarova YA and Borisy GG: Migration and actin protrusion in melanoma cells are regulated by EB1 protein. *Cancer Lett* 284: 30-36, 2009.
- Kim M-J, Yun HS, Hong E-H, Lee SJ, Baek JH, Lee CW, Yim JH, Kim JS, Park JK, Um HD, *et al*: Depletion of end-binding protein 1 (EB1) promotes apoptosis of human non-small-cell lung cancer cells via reactive oxygen species and Bax-mediated mitochondrial dysfunction. *Cancer Lett* 339: 15-24, 2013.
- Smith WL, DeWitt DL and Garavito RM: Cyclooxygenases: Structural, cellular, and molecular biology. *Annu Rev Biochem* 69: 145-182, 2000.
- Oshima M, Dinchuk JE, Kargman SL, Oshima H, Hancock B, Kwong E, Trzaskos JM, Evans JF and Taketo MM: Suppression of intestinal polyposis in Apc delta716 knockout mice by inhibition of cyclooxygenase 2 (COX-2). *Cell* 87: 803-809, 1996.
- Howe LR and Dannenberg AJ: A role for cyclooxygenase-2 inhibitors in the prevention and treatment of cancer. *Semin Oncol* 29: 111-119, 2002.
- Xu Z, Choudhary S, Voznesensky O, Mehrotra M, Woodard M, Hansen M, Herschman H and Pilbeam C: Overexpression of COX-2 in human osteosarcoma cells decreases proliferation and increases apoptosis. *Cancer Res* 66: 6657-6664, 2006.
- Kim JS, Chang JW, Yun HS, Yang KM, Hong EH, Kim DH, Um HD, Lee KH, Lee SJ and Hwang SG: Chloride intracellular channel 1 identified using proteomic analysis plays an important role in the radiosensitivity of HEp-2 cells via reactive oxygen species production. *Proteomics* 10: 2589-2604, 2010.

14. Yun HS, Baek J-H, Yim J-H, Lee SJ, Lee CW, Song JY, Um HD, Park JK, Park IC and Hwang SG: Knockdown of hepatoma-derived growth factor-related protein-3 induces apoptosis of H1299 cells via ROS-dependent and p53-independent NF- $\kappa$ B activation. *Biochem Biophys Res Commun* 449: 471-476, 2014.
15. Kim J-S, Kim EJ, Oh JS, Park I-C and Hwang S-G: CIP2A modulates cell-cycle progression in human cancer cells by regulating the stability and activity of Plk1. *Cancer Res* 73: 6667-6678, 2013.
16. Williams CS, Mann M and DuBois RN: The role of cyclooxygenases in inflammation, cancer, and development. *Oncogene* 18: 7908-7916, 1999.
17. Sobolewski C, Cerella C, Dicato M, Ghibelli L and Diederich M: The role of cyclooxygenase-2 in cell proliferation and cell death in human malignancies. *Int J Cell Biol* 2010: 215158, 2010. doi: 10.1155/2010/215158.
18. Munshi A and Ramesh R: Mitogen-activated protein kinases and their role in radiation response. *Genes Cancer* 4: 401-408, 2013.